Article ID: 1000-7032(2026)04-0672-08

A Compact LED-pumped Tri-wavelength Laser: Intracavity Seeding in A Hybrid Nd:YLF/Nd:YAG Cavity Without Wavelength Selectors

SHEN Jianping*, ZHANG Fengbo, DING Yi, XIA Ruize, ZUO Huanyu, HUANG Hao, ZHOU Shunyu

(*College of Electronic and Optical Engineering & College of Flexible Electronics, Nanjing University of Posts and Telecommunications, Nanjing* 210046, *China*)

* *Corresponding Author, E-mail: jianpingshen@njupt.edu.cn*

Abstract: This study presents a compact, LED-side-pumped laser based on a hybrid Nd:YLF/Nd:YAG gain medium that simultaneously generates output at 1 047, 1 053, 1 064 nm. Notably, this tri-wavelength operation is achieved without any intracavity wavelength-selective elements. In quasi-continuous-wave (QCW) mode at 20 Hz, the laser yielded an average power of 5.7 W. When actively *Q*-switched at 1 kHz, it produced 192 ns pulses with a peak power of 3.125 kW and a beam quality factor (M^2) of 5.3. To our knowledge, this work is the first to utilize an intracavity seeding injection technique to achieve multi-wavelength lasing, establishing a novel strategy for extending LED-pumped solid-state laser emission to adjacent spectral regions.

Keywords: LED-pumped; intracavity-seeding injection; multi-wavelength; acousto-optic modulator

CLC number: TN248.1 **Document code**: A

DOI: 10.37188/CJL.20250288 **CSTR**: 32170.14.CJL.20250288

一种基于无波长选择器的Nd:YLF/Nd:YAG复合腔内种子注入技术紧凑型LED泵浦三波长激光器

沈建平*, 张峰博, 丁 佚, 夏瑞泽, 左环宇, 黄 浩, 周顺禹

(南京邮电大学 电子与光学工程学院 & 柔性电子学院, 江苏 南京 210046)

摘要: 报道了一种基于混合Nd:YLF/Nd:YAG增益介质的紧凑型LED侧面泵浦固体激光器,实现1 047 nm、1 053 nm与1 064 nm三个波长的同步激光输出。值得注意的是,该三波长运转未使用任何腔内波长选择元件。在20 Hz准连续波工作模式下,激光器平均输出功率达到5.7 W;在1 kHz重复频率主动调*Q*运行时,实现脉冲宽度192 ns、峰值功率3.125 kW的激光输出,光束质量因子M^2为5.3。据我们所知,本研究首次采用腔内种子注入技术实现多波长激光输出,为LED泵浦固体激光器的工作波长拓展提供了一种新技术途径。

关 键 词: LED泵浦; 腔内种子注入; 多波长; 声光调制器

1 Introduction

Due to the unique advantage of simultaneously or alternately outputting multiple wavelengths, all-solid-state multi-wavelength lasers have a broader range of applications than single-wavelength lasers.

收稿日期: 2025-12-22; **修订日期**: 2026-01-07
基金项目: 南京邮电大学基金项目(KH1060325073, POCC2024M08, NY225119)
Supported by Nanjing University of Posts and Telecommunications Foundation (KH1060325073, POCC2024M08, NY225119)

They are particularly valuable in fields such as air pollution detection, blood testing, medical applications, differential absorption lidar, and terahertz wave generation[1-2]. Currently, the main technical approaches for tri-wavelength lasers include: nonlinear frequency conversion (such as frequency doubling and sum-frequency generation)[3], disordered crystal gain media (such as Yb, Y: CaF_2, Yb: YAB, and other materials with broad emission spectra)[4], and cavity loss tuning techniques (where resonator losses are adjusted to balance the gain competition between different wavelengths)[5]. Each technique has its advantages and disadvantages: nonlinear frequency conversion offers high efficiency but results in a complex system; disordered crystals have broad spectral characteristics but suffer from significant reabsorption losses; cavity loss tuning allows wavelength tunability but has lower efficiency and requires high precision in system design and adjustment.

With the widespread application of LEDs in the lighting and manufacturing industries, LEDs have gradually become a strong alternative to laser diode (LD) pump sources for all-solid-state lasers due to their excellent emission characteristics, compact design, and long lifespan. In particular, compared to LDs, LEDs have a broader emission spectrum, which matches well with the absorption spectrum of laser gain media, thereby improving pumping efficiency. The pumping distribution of LEDs is more uniform, reducing the thermal lensing effect caused by localized heat accumulation. Furthermore, with advancements in technology, the optical power of individual LED chips has reached the wattage level, and production costs have significantly decreased, driving the rapid development of LEDs in laser applications. Up to the present, LED-based pumping has been successfully applied to single-wavelength lasers such as Nd:YAG[6-10], Ce: Nd:YAG[11-12], Nd: YLF[13-14], and Nd:glass[15-16]. However, the Lambertian emission characteristics of LEDs result in lower pumping density and larger radiation angles, making it difficult to focus the optical flux into a small pumping volume, especially when precisely coupled with a laser resonator (such as in the TEM_{00} mode). As a result, existing research has yet to fully explore the potential of LEDs in multi-wavelength laser systems, particularly in terms of spectral modulation and uniform distribution of pump power, where significant limitations still exist.

To address the limitations of conventional multi-wavelength lasers, such as low LED pumping efficiency and high system complexity, this study demonstrates an innovative actively Q-switched laser based on a side-pumped dual-rod configuration with Nd: YAG and Nd: YLF. The design incorporates three key features. Firstly, the hybrid gain medium produces a composite spectrum covering the 1 047 nm, 1 053 nm, and 1 064 nm transitions. The intense 1 064 nm laser field generated from the Nd: YAG rod interacts intracavity with the Nd: YLF rod, seeding and rapidly bringing the 1 053 nm transition to threshold. Secondly, the partially non-overlapping gain profiles of the two media help suppress mode competition. Each crystal predominantly amplifies its respective wavelength, thereby significantly improving the stability of simultaneous multi-wavelength operation. Finally, by optimizing the pumping parameters and adopting a water-cooled modular architecture, stable simultaneous tri-wavelength laser output has been successfully achieved.

2　Experiment Setup

Fig. 1 illustrates the structure of an acousto-optic (A—O) Q-switched all-solid-state narrow-pulse multi-wavelength laser operating at 1 047 nm, 1 053 nm, and 1 064 nm. The laser resonator is constructed with an LED side-pumped Nd:YLF module and an Nd:YAG module arranged in series with a Q-switch. Firstly, the gain modules share a similar design. The Nd:YLF rod (ϕ6.2 mm×95 mm, 1.0% Nd^{3+}(at.)) and the Nd:YAG rod (ϕ5 mm×120 mm, 1.0% Nd^{3+}(at.)) are each housed in a dedicated water-cooled chamber. The Nd:YLF module is pumped by five rows of LED arrays (15 beads per array), symmetrically arranged around the rod. Each LED bead emits at a center wavelength of 810 nm (FWHM: ~30 nm) with a 90° beam angle. Similarly,

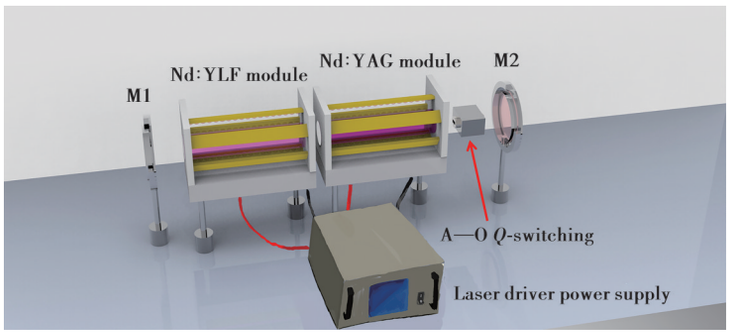

Fig.1 Experimental setup for the LED-pumped A—O tri-wavelength Q-switched laser

the Nd:YAG module is pumped by an array of 20 LED beads. Both the crystals and LED arrays are actively cooled, with the crystal cooling water maintained at ~18 ℃ and the LED arrays embedded in copper blocks held at ~5 ℃ to ensure stability. The LEDs are driven in a QCW mode at 20 Hz with a 10 ms pulse width to optimize pumping efficiency and uniformity while mitigating thermal effects. The core advantage of this solution lies in reducing the average input power to 20% of that in continuous-wave drive, thereby significantly minimizing heat generation at the source. Simultaneously, the extended 40-millisecond pulse interval provides ample thermal relaxation time for the LED chip, allowing heat to dissipate effectively through the heat sink before the next pulse arrives and preventing thermal buildup. Secondly, the optical cavity, with a total length of 430 mm, is defined by two mirrors. The rear mirror (M1) has a high-reflectivity (HR) coating (R>99.9%) across the 1 045–1 065 nm band, while the output coupler (M2) features a partial-transmission coating with specified transmittances of 7.6%, 7.8%, and 10.2% within the same wavelength range. Finally, the pulsed operation is achieved using a 1 064 nm A—O Q-switch (I-QS027-5C4G, Gooch & Housego) positioned near M2, which is driven by its dedicated RF (repetition frequency) generator at 27.12 MHz and up to 50 W of power.

3 Experimental Results and Discussions

This study theoretically investigates the feasibility of achieving tri-wavelength output at 1 047, 1 053, 1 064 nm from a series-integrated Nd:YLF/Nd:YAG laser. We perform numerical simulations to assess the intracavity intensity distribution and establish a comprehensive theoretical model that integrates the key spectroscopic parameters of both media to characterize the laser system's threshold condition.

$$\frac{\mathrm{d}N_2}{\mathrm{d}t} = R_\mathrm{p}(t) - \frac{N_2}{\tau_{21}} - v_\mathrm{g}\Gamma_\mathrm{l}\left[g_1 S_1 + g_2 S_2\right] - W_{22}N_2^2, \tag{1}$$

$$\frac{\mathrm{d}S_1}{\mathrm{d}t} = v_\mathrm{g}\Gamma_1 g_1 S_1 - \frac{S_1}{\tau_{\mathrm{p}1}} + \beta_1\frac{N_2}{\tau_{21}}, \tag{2}$$

$$\frac{\mathrm{d}S_2}{\mathrm{d}t} = v_\mathrm{g}\Gamma_1 g_2 S_2 - \frac{S_2}{\tau_{\mathrm{p}2}} + \beta_2\frac{N_2}{\tau_{21}}, \tag{3}$$

in these Eqs. (1), (2) and (3), we have defined the rate equations. In Eq. (1), we present the upper-level population inversion density. In Eqs. (2) and (3), we give the photon densities corresponding to the two spectral lines of Nd:YLF, respectively. The physical meanings of the symbols in Eqs. (1) through (3) are defined as follows. The variable N_2 denotes the population inversion density of the upper laser level. The pump rate, $R_\mathrm{p}(t)$, represents the number of particles excited to the upper level per unit time and volume. The fluorescence lifetime of the upper level is given by τ_{21}. The group velocity of photons within the resonator cavity is v_g. The optical confinement factor, Γ_l, characterizes the overlap efficiency between the laser mode volume and the physical volume of the gain medium. The gain coefficients for the respective laser transitions are g_1 and g_2. The photon densities for the two spectral lines are S_1 and S_2. The coefficient W_{22} accounts for the rate of nonlinear losses due to effects such as excited-state absorption or energy-transfer upconversion. The photon lifetime within the cavity for the two

wavelengths is τ_{p1} and τ_{p2}. Finally, β_1 and β_2 are the spontaneous emission factors, indicating the fraction of spontaneous radiation coupled into the respective laser modes. Based on the above set of rate equations, we derive the following Eqs. to characterize the parameters of a multi-wavelength laser. Based on the rate equations above, we have derived Eqs. (4) and (5):

$$P_{k,i}(\tau_F) = \max\left[\eta_{ext}\frac{h\nu_i V_{eff}}{\tau_{p,i}} S_i(t:\tau_F)\right], \quad (4)$$

$$E_i(\tau_F) = \eta_{ext}\frac{h\nu_i V_{eff}}{\tau_{p,i}}\int S_i(t:\tau_F)\mathrm{d}t, \quad (5)$$

in these Eqs. (4) and (5), indices $i = 0$ and 1 correspond to the emission wavelengths of 1 047 nm and 1 053 nm, respectively. $P_{k,i}(\tau_F)$ represents peak power of the Nd:YLF and Nd:YAG laser crystals; $E_i(\tau_F)$ represents pulse energy of the Nd:YLF and Nd:YAG laser crystals; η_{ext} represents output coupling efficiency; h represents Planck constant, ν_i represents the frequency of the laser; V_{eff} represent effective mode volume; $\tau_{p,i}$ represents the fluorescence lifetime of the upper laser level in Nd:YLF and Nd:YAG laser crystals; S_i represents the photon density. By combining the rate equations, we can solve for $S_i(t:\tau_F)$:

$$\eta_{ext,i} = \frac{\alpha_{m,i}}{\alpha_i + \alpha_{m,i}}, \quad (6)$$

$$\alpha_{m,i} = \frac{1}{2L}\ln\frac{1}{R_{1,i}R_{2,i}}, \quad (7)$$

in these Eqs. (6) and (7), $\alpha_{m,i}$ represents output coupling loss; L represents the length of cavity; R represents reflectivity of the lens. These formulas can demonstrate the trends of 1 047 nm, 1 053 nm, and 1 064 nm as the pump width changes. The above formulas demonstrate the trend of peak energy variation with repetition rate for Nd:YLF and Nd:YAG tri-wavelength lasers, with the results presented in the Fig. 2.

The theoretical simulation results of the dependence of laser peak energy on pulse repetition frequency is presented in Fig. 2. To enhance the readability of the data plots, we used the pump FWHM (full width at half maximum) as the horizontal axis (X-axis), since this parameter is directly proportional

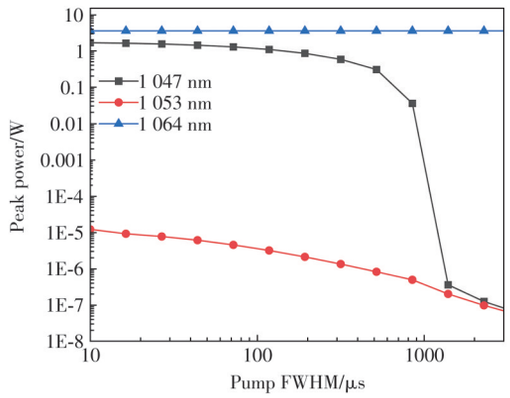

Fig.2　The peak power of Nd:YLF and Nd:YAG laser at various pump FWHM

to the frequency. The data reveal a distinct trend: as the repetition rate increases, the peak energies at 1 047 nm and 1 053 nm decrease progressively, whereas the 1 064 nm output remains comparatively stable. This phenomenon can be explained by Eqs. (4) and (5). A higher repetition rate reduces the intracavity power density, to which the 1 047 nm and 1 053 nm transitions (originating from the Nd:YLF gain medium) are highly sensitive. The 1 064 nm line, however, benefits from a lower threshold in the Nd:YAG medium, making its output more resilient to such changes.

Fig. 3 presents the experimentally measured, normalized emission spectra of the laser at different drive frequencies, measured under a constant average current of 1.2 A using a spectrometer (Ocean Optics HR4000, resolution: 0.02 nm). The spectra demonstrate that the output wavelengths are effectively controlled by the pump and frequency modulation.

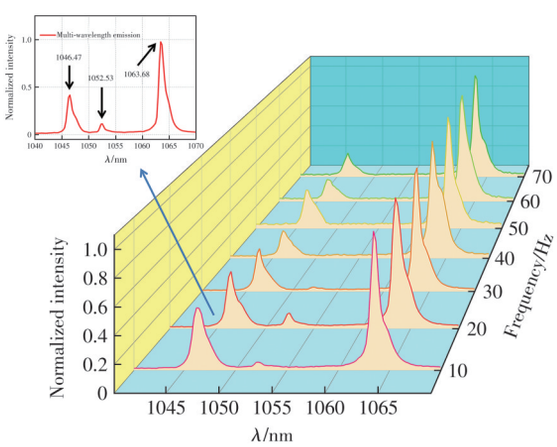

Fig.3　The emission spectra of Nd:YLF and Nd:YAG double rods in the QCW mode laser operation

Simultaneous lasing at 1 046.47 nm, 1 052.53 nm, and 1 063.68 nm is clearly observed at drive frequencies between 10 Hz and 20 Hz. However, this multi-wavelength operation becomes less distinct above 30 Hz. This transition is attributed to the favorable conditions at lower frequencies, including reduced thermal lensing and weaker gain competition, which collectively support concurrent oscillation at multiple wavelengths. As the frequency increases, the broader pump pulse width (FWHM) leads to a decrease in the intensities of the 1 047 nm and 1 053 nm lines from Nd∶YLF, a trend that is consistent with the data presented in Fig. 2.

Fig. 4 presents the output power characteristics of the multi-wavelength laser in QCW operation as a function of the output coupler transmittance. The system achieves a maximum output power of 5.7 W at a coupling transmittance of 10.2%, under a pump power of 58.7 W and a repetition rate of 20 Hz. This operating point corresponds to a maximum optical conversion efficiency of 10.52% and a slope efficiency of 12%. Notably, the laser output does not exhibit saturation at this transmittance, indicating that further optimization of the output coupler design and its precise matching with the pump power can lead to even higher conversion efficiency, as well as improved system stability and reliability.

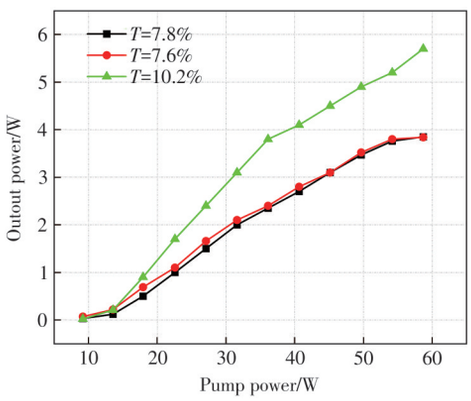

Fig.4 Average output power of the tri-wavelength laser as a function of pump power in the QCW regime

After testing the parameters of the laser in QCW mode, we measured the pulse waveform of the laser modulated by A—O Q-switching. The temporal pulse profile is recorded using a fast photodiode (Thorlabs PDA10A2) and a digital oscilloscope (Tektronix MDO3034). As shown in Fig. 5, both the long-term pulse train and a single pulse from the tri-wavelength Q-switched laser are displayed. The single pulse exhibits a characteristic double-peak structure, a phenomenon attributed to the distinct upper-state lifetime of the Nd∶YAG and Nd∶YLF gain media. Nd∶YAG, with a shorter upper-state lifetime of ~230 μs, releases its stored energy rapidly upon the opening of the A—O Q-switch, forming the first and stronger peak. In contrast, Nd∶YLF, with a longer upper-state lifetime of ~480 μs, releases its energy more slowly, resulting in a delayed and slightly smaller second peak. Thus, the temporal separation of the two peaks directly results from the different energy release dynamics of the two gain media. Due to the relatively low output power of the 1 053 nm laser from the Nd∶YLF crystal, only two peaks could be detected on the oscilloscope.

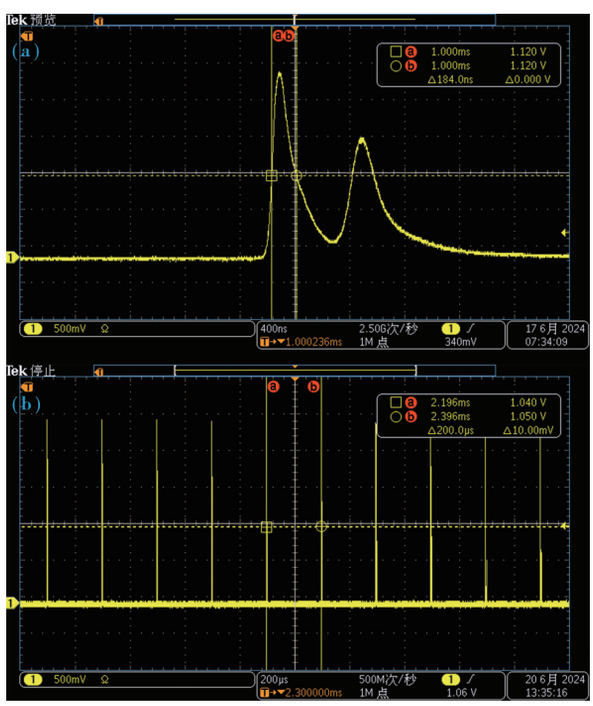

Fig.5 (a)The separately pulse Q-switched tri-wavelength laser. (b)The temporal profile of the pulse sequence

Fig. 6(a) and 6(b) summarize the average output power and pulse width of the tri-wavelength Q-switched laser as a function of modulation frequency for an output coupler with T=7.8%. As the frequency increases from 500 Hz to 10 kHz, the average output power rises from 0.274 W to 2 W. In Q-switched

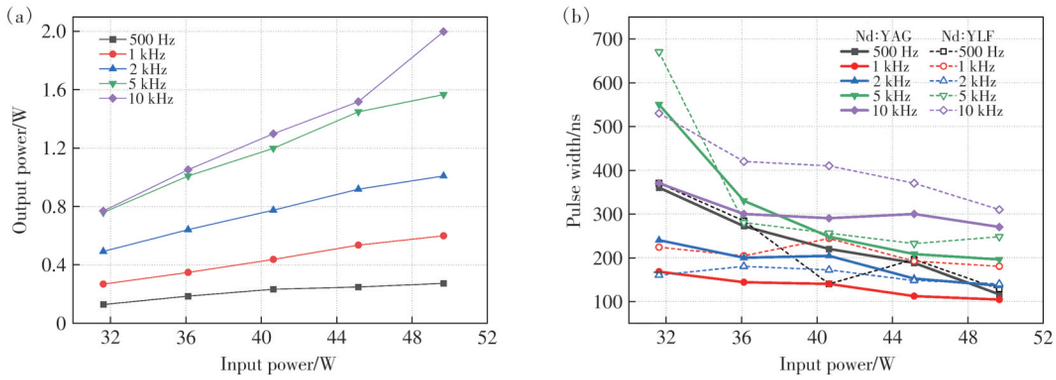

Fig.6　(a)Average power and (b)pulse width in relation to pump power at various repetition frequencies with AO modulation

operation, a peak power of 3. 125 kW is achieved at 1 kHz, with a corresponding pulse energy of 0. 6 mJ and a pulse duration of 192 ns. This data underscores the significant role of modulation frequency in shaping pulse characteristics, illustrating that precise frequency adjustment offers an effective means for pulse compression and laser performance optimization.

Fig. 7 presents the spatial energy distribution near the laser beam waist at medium output power for (a) QCW and (b) *Q*-switched operation modes, with the insets showing the corresponding transverse mode patterns. The data, captured by a Cinogy CMOS-1201 beam profiler at various positions, were used to determine the beam quality factors *via* least-squares curve fitting. The M^2 factors for the QCW laser are 7. 5 and 7. 2 in the *x* and *y* directions, respectively, while those for the *Q*-switched laser are 5. 3 and 5. 5. The superior beam quality in *Q*-switched mode is attributed to its short pulse duration, which minimizes thermal accumulation and associated effects like thermal lensing. Conversely, in QCW mode, the prolonged pulse width leads to significant heat buildup, particularly in the Nd∶YLF crystal due to its longer fluorescence lifetime and lower thermal conductivity, thereby degrading beam quality and inducing modal instability.

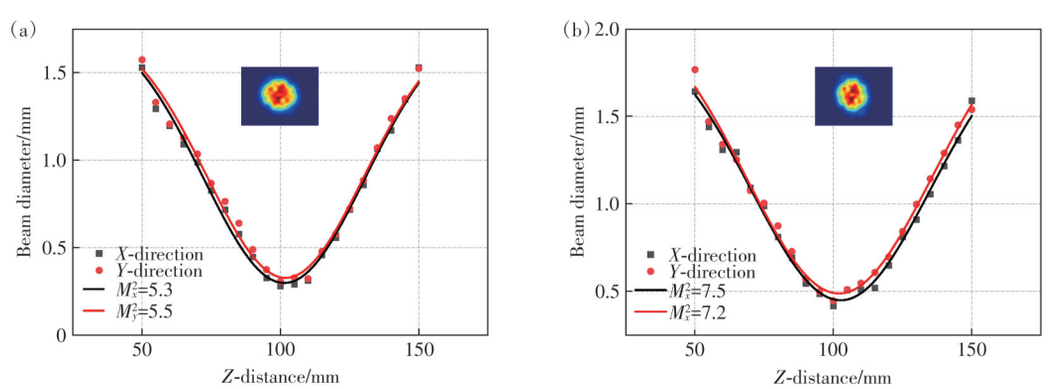

Fig.7　Beam quality and 2-dimensional laser beam profiles of the laser beam for (a)QCW operation and (b)*Q*-switched operation

Fig. 8 depicts the average power stability of the multi-wavelength laser in *Q*-switched operation, quantified by the root mean square (RMS) stability of below 3. 5% over a 30 minute sampling period. The observed power fluctuations are primarily attributed to the thermal dynamics of the system, which can be analyzed from two perspectives. First, heat generation from the LED pump source during prolonged operation causes a redshift in its emission spectrum due to bandgap narrowing. This spectral shift moves the peak wavelength away from the optimal absorption band of the gain media, thereby reducing pumping efficiency. Additionally, elevated temperature enhances non-radiative recombination in the LEDs, further decreasing their optical output and introducing pump power instability. Second, thermal effects within the solid-state gain media themselves exacerbate the issue. The absorbed pump energy that is converted to heat creates a temperature gradient, inducing thermal lensing. This

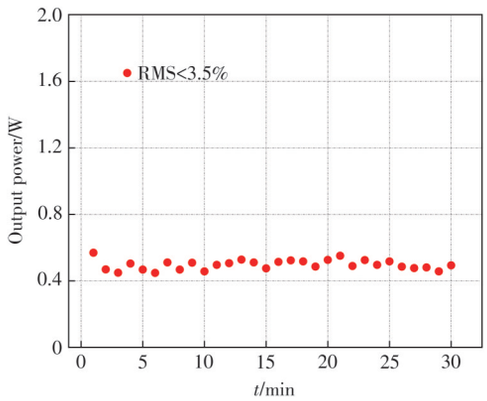

Fig.8 Stability of the tri-wavelength Nd∶YLF and Nd∶YAG laser in *Q*-switching mode

effect alters the refractive index, distorts the beam profile, and degrades mode matching within the resonator. Furthermore, thermal stress can induce changes in the physical cavity length, compromising resonator stability and leading to additional output power variations.

4 Conclusion

In conclusion, this work successfully demonstrates an actively *Q*-switched, tri-wavelength (1 047/1 053/1 064 nm) laser based on a hybrid Nd∶YLF/Nd∶YAG gain medium and LED side-pumping, all achieved without intracavity wavelength-selective elements. The innovative incorporation of intracavity seeding within the dual-rod configuration was pivotal in reducing the oscillation threshold and enhancing the pump power density. The laser's performance was validated through two operational modes: in QCW mode at 20 Hz, it delivered 5.7 W of average power, and in *Q*-switched mode at 1 kHz, it produced 192 ns pulses with a peak power of 3.125 kW and a beam quality factor of M^2=5.3. To the best of our knowledge, this represents the first implementation of an actively *Q*-switched, LED-pumped tri-wavelength laser utilizing this hybrid crystal approach. This study thus establishes a new, cost-effective strategy for developing compact and efficient all-solid-state lasers operating at multiple wavelengths.

Response Letter is available for this paper at: http://cjl.lightpublishing.cn/thesisDetails#10.37188/CJL.20250288

References:

[1] TU Z H, DAI S B, ZHU S Q, *et al*. Efficient high-power orthogonally-polarized dual-wavelength Nd∶YLF laser at 1 314 and 1 321 nm [J]. *Opt. Express*, 2019, 27(23): 32949-32957.

[2] ZUO Z Y, DAI S B, ZHU S Q, *et al*. Power scaling of an actively *Q*-switched orthogonally polarized dual-wavelength Nd∶YLF laser at 1 047 and 1 053 nm [J]. *Opt. Lett.*, 2018, 43(19): 4578-4581.

[3] WANG Z C, YANG F, XIE S Y, *et al*. Multiwavelength green-yellow laser based on a Nd∶YAG laser with nonlinear frequency conversion in a LBO crystal [J]. *Appl. Opt.*, 2012, 51(18): 4196-4200.

[4] LI C, LIU J, SU L B, *et al*. Diode-pumped tri-wavelength synchronously mode-locked Yb, Y∶CaF_2 laser [J]. *Appl. Opt.*, 2015, 54(32): 9509-9512.

[5] SI Z Z, DAI C Q, LIU W. Tunable three-wavelength fiber laser and transient switching between three-wavelength soliton and *Q*-switched mode-locked states [J]. *Chin. Phys. Lett.*, 2024, 41(2): 020502.

[6] CHO C Y, PU C C, CHEN Y F, *et al*. Energy scale-up and mode-quality enhancement of the LED-pumped Nd∶YAG *Q*-switched laser achieving a millijoule green pulse [J]. *Opt. Lett.*, 2019, 44(13): 3202-3205.

[7] JIANG R R, JIANG S T, XU S C, *et al*. Watt-level LED-pumped actively *Q*-switched 1 319 nm laser with high repetition rate operation [J]. *Opt. Mater.*, 2024, 147: 114756.

[8] SHEN J P, HUANG X, XU S C, *et al*. High average power green laser based on LED-side-pumped *Q*-switched Nd∶YAG laser [J]. *IEEE Photonics Technol. Lett.*, 2023, 35(13): 721-724.

[9] PICHON P, BARBET A, BLENGINO D, *et al*. High-radiance light sources with LED-pumped luminescent concentrators applied to pump Nd∶YAG passively *Q*-switched laser [J]. *Opt. Laser Technol.*, 2017, 96: 7-12.

[10] SHEN J P, CHEN Y, CHEN L, *et al*. A high peak power passively *Q*-switched Nd∶YAG dual-rod 532 nm laser based on LED side pumping [J]. *Chin. Phys. Lett.*, 2025, 42(4): 044202.

[11] VILLARS B, HILL E S, DURFEE C G. Design and development of a high-power LED-pumped Ce∶Nd∶YAG laser [J].

Opt. Lett., 2015, 40(13): 3049-3052.

[12] SHEN J P, XING F Y, CHEN Y, *et al.* LED-side-pumped quasi-CW and passively *Q*-switched single longitudinal mode laser based on a twist-mode cavity [J]. *Opt. Laser Technol.*, 2025, 186: 112783.

[13] ZHAO T Z, XIAO H, GE W Q, *et al.* Light-emitting-diode-pumped active *Q*-switched Nd:YLF laser [J]. *Opt. Lett.*, 2019, 44(8): 1956-1959.

[14] SHEN J P, CHEN L, CHEN Y, *et al.* Dual-wavelength *Q*-switched LED-pumped lasers: hybrid Nd:YLF/glass dual-rod injection seeding [J]. *IEEE Photonics Technol. Lett.*, 2025, 37(22): 1281-1284.

[15] NOURRY-MARTIN M, FERMON N, LE BLANC C, *et al.* Indirectly LED-pumped Nd:glass: potential for high energy laser facilities [J]. *Optica*, 2025, 12(3): 311-314.

[16] SHEN J P, LU P, XU S C, *et al.* First demonstration of watt-level LED-pumped actively *Q*-switched Nd:glass rod laser [J]. *Appl. Phys.* B, 2024, 130(5): 69.

沈建平(1980–),男,山东临沂人,博士,副教授,硕士生导师,2014年于北京交通大学获得博士学位,主要从事全固态LED/LD泵浦激光器系统及其应用的研究。

E-mail: jianpingshen@njupt.edu.cn